

In this paper, we report the analysis and structural elucidation of a new sildenafil analogue, cyclopentynafil and a new tadalafil analogue, *N*-octylnortadalafil, that were isolated from a dietary supplement illegally marketed for erectile dysfunction.

Experimental

Chemicals and Reagents HPLC-grade acetonitrile and all other reagents (analytical grade) were purchased from Wako Pure Chemical Industries, Ltd. (Osaka, Japan).

Sample The examined product was purchased as a processed food composed mainly of walnuts through the Internet and was composed of four pieces of ivory tablets (400 mg). The product properties were as follows: product name; Highperwalnut 2, producing company; Art Creation Co., Ltd., sales company; Ogawa Planning Co., Ltd., date of purchase; December 28, 2007.

Preparation of Sample Solution One tablet was finely powdered, and 100 mg of the powder was ultrasonically extracted in 10 ml of 70% methanol for 15 min. The extract was centrifuged at 1700×g. The supernatant was filtered through a 0.45 μm filter. The filtrate was used for HPLC, and a portion of it was diluted 10-fold with methanol for liquid chromatography-electrospray ionization-mass spectrometry (LC-ESI-MS) analysis.

HPLC Analysis HPLC analysis was performed using a JASCO PU-2089 apparatus equipped with a photodiode array (PDA) detector model MD-2015 (JASCO Corporation, Tokyo, Japan). The sample solution was separated by using a TSK-GEL ODS-80Ts column (150×4.6 mm i.d., 5 μm, Tosoh Co., Tokyo, Japan). The mobile phase was an acetonitrile/water/phosphoric acid (100:900:1) mixture solution containing 5 mmol/l sodium hexanesulfonate (eluent A) and an acetonitrile/water/phosphoric acid (900:100:1) mixture solution containing 5 mmol/l sodium hexanesulfonate (eluent B). The gradient elution was started at 90% eluent A, and was linearly decreased to 55% A in 25 min and to 10% A in 44–49 min. The flow rate of the mobile phase was set at 1.0 ml/min, and the injection volume was 20 μl. The column temperature was maintained at 40 °C. The PDA detection wavelength was set from ultraviolet (UV) 200 to 400 nm, and max-plot chromatographic monitoring was performed (200–400 nm).

LC-ESI-MS Analysis LC-ESI-MS analysis was performed using a Waters alliance 2695 separation module and ZQ mass spectrometer (Waters Corporation, Milford, MA, U.S.A.). The sample solution was separated by using an Atlantis dC18 column (150×2.1 mm i.d., 3 μm, Waters Corporation). The mobile phase was 0.1% formic acid aqueous solution (eluent A) and acetonitrile containing 0.1% formic acid (eluent B). The gradient elution began at 95% eluent A, and linearly decreased to 80% A in 15 min and to 20% A in 30–35 min. The flow rate of the mobile phase was set at 0.2 ml/min, and the injection volume was 10 μl. The column temperature was maintained at 40 °C. ESI on both positive and negative modes was used for the analysis. The instrument parameters were as follows: source temperature, 120 °C; desolvation temperature, 350 °C; capillary voltage, 3 kV; cone voltage, 30, 60 V (ESI positive), -60 V (ESI negative); and desolvation gas flow, 600 l/h. The mass range of the spectra was *m/z* 100 to *m/z* 800.

Isolation of Compounds 1 and 2 Sample powder (300 mg) was dissolved in 20 ml water, and the solution was extracted with 40 ml diethyl ether for 10 min, three times. All of the diethyl ether layers were combined, dehydrated with anhydrous sodium sulfate for 1 h, and filtrated by filter paper. The filtrate was evaporated to dryness then reconstituted with 3 ml methanol. The methanol solution was centrifuged, and the precipitate was dried *in vacuo* to afford compound 1 (18.8 mg). The supernatant was applied to silica gel 60F₂₅₄ TLC plates (20×10 cm with 1.0 mm thickness, Merck, Darmstadt, Germany) in a band. The plates were developed using a saturated tank with a hexane/ethyl acetate/acetic acid mixture (50:50:1) to a distance of about 7 cm. After air-drying, the plates were examined using UV light (wavelength: 254 nm). A band with an *R_f* value of 0.39 was scraped and dissolved in 120 ml of methanol. The methanol solution was filtered, and the filtrate was evaporated to dryness. The residue was reconstituted in 10 ml diethyl ether. This solution was filtered, and the filtrate was evaporated to dryness to afford compound 2 (4.4 mg).

Measurement of Accurate Mass The accurate mass of the target compound was measured by the LTQ Orbitrap XL instrument (Thermo Fisher Scientific Inc., Waltham, MA, U.S.A.) with the direct-infusion ESI positive-ion mode under the following conditions: solvent flow rate 5 μl/min, sheath gas flow rate 20 arb, aux gas flow rate 10 arb, spray voltage 5 kV, capillary temperature 275 °C, capillary voltage 4 V, and tube lens 60 V. Tyrosine 1, 3, 6 standard was used as a mass calibrant of FT mass analyzer (resolu-

tion=100000), and tyrosine 3 standard was used as a lock mass ion (*m/z* 508.20783) during the measurement. Theoretical mass and delta value (*mmu*) were calculated by using the elemental composition tool of Xcalibur/Qual Browser software.

NMR Analysis CDCl₃ (99.96%) and CD₃OD (99.96%) were purchased from ISOTEC Inc., which is part of Sigma-Aldrich Inc. (St. Louis, MO, U.S.A.). The NMR spectra were obtained on an ECA-800 spectrometer (JEOL Ltd., Tokyo, Japan) equipped with HCNFG and CH5FG probes (JEOL Ltd.). The ¹H- and ¹³C-NMR chemical shifts of compounds 1 and 2 were assigned by heteronuclear multiple quantum coherence (HMQC), heteronuclear multiple-bond correlation (HMBC), ¹H-¹H shift correlation spectroscopy (¹H-¹H COSY) and nuclear Overhauser effect (NOE) spectra.

Measurement of Circular Dichroism The circular dichroism (CD) spectra of compound 2 and tadalafil were measured by using a J-720 spectropolarimeter (JASCO Corporation, Tokyo, Japan) with a quartz cell 10 mm in length. The concentration in methanol solution of compound 2 and tadalafil were 0.041 mmol/l and 0.044 mmol/l, respectively.

Docking Study of Compounds 1 and 2 with PDE-5 Docking models of compounds 1 and 2 bound to PDE-5 were constructed by conformational search simulation (Mixed MCMM/Low Mod). AMBER* was used as force field. Calculations were performed by MacroModel (ver. 8.1). IUDT (PDB ID) and IUDU, crystal structures of PDE-5 were used for docking models of compounds 1 and 2, respectively.

Results and Discussion

In this study, we reported 1 and 2 as newly isolated compounds from an illegal dietary supplement. Figure 2A shows the HPLC chromatograms of an extract of the supplement. Two main peaks were detected in the extract, one at 20.9 min (compound 1) and the other at 37.2 min (compound 2). The PDA-sliced UV spectrum of 1 exhibited a quite similar profile (*λ*_{max} nm: 218, 290, Fig. 2B) to that of sildenafil; however, 1 eluted at a later retention time (20.9 min) than sildenafil (18.3 min) under the same chromatographic conditions. Meanwhile, the PDA-sliced UV spectrum of 2 showed a quite similar profile (*λ*_{max} nm: 281, Fig. 2C) to tadalafil, but 2 eluted at a later retention time (37.2 min) than tadalafil

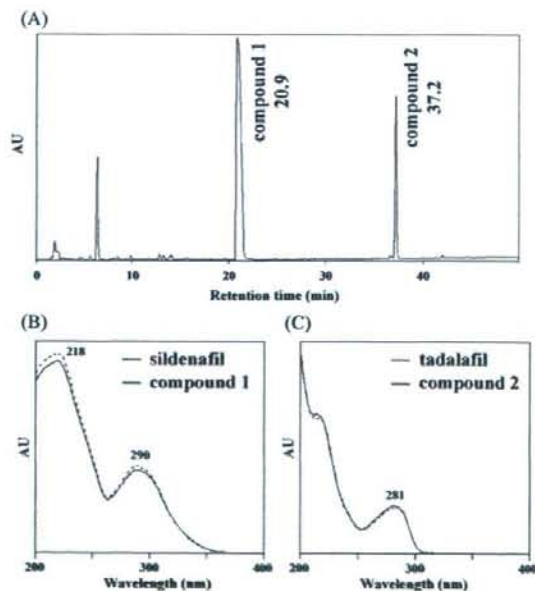


Fig. 2. (A) HPLC Chromatogram of the Sample Solution Monitored Max Plot (200–400 nm) and (B) the Overlaid UV Spectra of Sildenafil and Compound 1, and (C) the Overlaid UV Spectra of Tadalafil and Compound 2

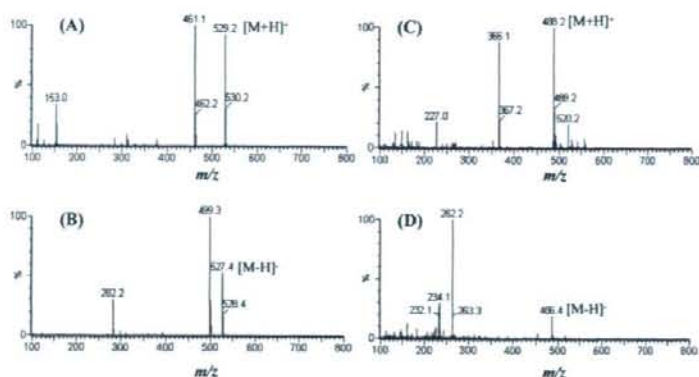


Fig. 3. Mass Spectra of Compounds **1** and **2** by LC-ESI-MS Analysis

(A) Compound **1** (positive, cone voltage: 60 V), (B) compound **1** (negative, cone voltage: -60 V), (C) compound **2** (positive, cone voltage: 30 V), (D) compound **2** (negative, cone voltage: -60 V).

(20.0 min). Furthermore, the peak of **1** exhibited major ion peaks at m/z 529 $[M+H]^+$ in the positive scan mode and at m/z 527 $[M-H]^-$ in the negative scan mode by LC-ESI-MS analysis (Figs. 3A,B). Also major ion peaks at m/z 488 $[M+H]^+$ and at m/z 486 $[M-H]^-$ were detected in the peak of **2** (Figs. 3C,D). These data strongly suggested that **1** is a sildenafil analogue and **2** a tadalafil analogue.

Compound **1** formed a colorless amorphous powder and was determined by accurate mass measurement to have the molecular formula $C_{26}H_{36}N_6O_4S$ with a quasimolecular ion at m/z 529.2590 (Calcd 529.2597) $[M+H]^+$. The 1H -NMR spectrum of **1** exhibited 35 nonexchangeable protons, including a methyl signal at 4.28 (3H, s), an ethoxyl group of signals at 1.65 (3H, t, $J=6.9$ Hz), 4.37 (2H, q, $J=6.9$ Hz), a *n*-propanyl group of signals at 1.01 (3H, t, $J=7.3$ Hz), 1.86 (2H, sext, $J=7.3$ Hz), 2.92 (2H, t, $J=7.3$ Hz) and ABX-type aromatic proton signals at 7.14 (1H, d, $J=8.7$ Hz), 7.83 (1H, dd, $J=2.3, 8.7$ Hz), 8.83 (1H, d, $J=2.3$ Hz). The ^{13}C -NMR spectrum of **1** showed 3 methyls, 11 methylenes, including an oxygenated carbon (66.1), 4 methines including 3 aromatic carbons (113.0, 131.3, 131.8) and 7 aromatic quaternary carbons (121.1, 124.5, 128.6, 138.4, 146.4, 147.0, 159.3), and a carbonyl group (153.6). These signals are very similar to those of sildenafil (Table 1), except for the disappearance of an *N*-methyl group and the presence of a methine signal at 2.51 (1H, quint, $J=7.6$ Hz) and two sets of equivalent methylene signals at 1.53 (2H, m) and 1.63 (2H, m), and 1.28 (2H, m) and 1.83 (2H, m).

Interpretation of the 1H - 1H COSY and HMQC spectra of **1** indicated the presence of a cyclopentyl group (Fig. 4). The connectivity of this group was deduced from the HMBC spectrum (Fig. 4). The methine proton at 2.51 (H-29) of the cyclopentyl group showed correlations to the methylene carbons at 51.2 (C-25, C-27) of sildenafil. These data determined the structure of **1** as 5-[2-ethoxy-5-(4-cyclopentylpiperazin-1-ylsulfonfyl)phenyl]-1-methyl-3-propyl-1,6-dihydro-7H-pyrazolo[4,3-*d*]pyrimidin-7-one. The assignments of the 1H - and ^{13}C -NMR signals of **1** are summarized in Table 1. Considering its properties, compound **1** is named as cyclopentynafil.

Compound **2** formed a colorless amorphous powder and was determined by accurate mass measurement to have the

Table 1. 1H - and ^{13}C -NMR Chemical Shifts of Compound **1** and Sildenafil in $CDCl_3$

Position	1 ($^1H^a$)	Sildenafil ($^1H^a$)	1 ($^{13}C^b$)	Sildenafil ($^{13}C^b$)
1			147.0	146.4
4			153.6	153.6
5	10.80 s	10.82 s		
6			146.4	147.0
8			138.4	138.4
9			124.5	124.5
10 (3H)	4.28 s	4.28 s	38.2	38.2
11 (2H)	2.92 t (7.3)	2.93 t (7.2)	27.8	27.7
12 (2H)	1.86 sext (7.3)	1.86 sext (7.2)	22.3	22.2
13 (3H)	1.01 t (7.3)	1.02 t (7.2)	14.0	14.0
14			121.1	121.1
15	8.83 d (2.3)	8.82 d (2.4)	131.3	131.2
16			128.6	129.0
17	7.83 dd (2.3, 8.7)	7.84 dd (2.4, 8.6)	131.8	131.7
18	7.14 d (8.7)	7.15 d (8.6)	113.0	113.0
19			159.3	159.3
20 (2H)	4.37 q (6.9)	4.37 q (6.9)	66.1	66.1
21 (3H)	1.65 t (6.9)	1.65 t (6.9)	14.6	14.5
24 (2H)	3.10 brs	3.11 brs	46.1	45.9
25 (2H)	2.59 brs	2.50 brs	51.2	54.0
27 (2H)	2.59 brs	2.50 brs	51.2	54.0
28 (2H)	3.10 brs	3.11 brs	46.1	45.9
29	2.51 quint (7.6)	2.28 (3H) s	66.8	45.7
30 (2H)	1.28 m, 1.83 m		30.4	
31 (2H)	1.53 m, 1.63 m		24.0	
32 (2H)	1.53 m, 1.63 m		24.0	
33 (2H)	1.28 m, 1.83 m		30.4	

a) Recorded in 800MHz and J values (in Hz) in parentheses. b) Recorded in 200MHz.

molecular formula $C_{25}H_{33}N_3O_4$ with a quasimolecular ion at m/z 510.2362 (Calcd 510.2363) $[M+Na]^+$. The 1H -NMR spectrum of **2** exhibited 32 nonexchangeable protons, including a methyl signal at 0.89 (3H, t, $J=7.3$ Hz), a methylenedioxy group signal at 5.85 (2H, d, $J=6.9$ Hz), ABX-type aromatic proton signals at 6.68 (1H, d, $J=7.8$ Hz), 6.78 (1H, d, $J=1.9$ Hz) and 6.79 (1H, dd, $J=7.8, 1.9$ Hz), and AB-type aromatic proton signals at 7.02 (1H, brt, $J=7.8$ Hz), 7.07 (1H, brt, $J=8.2$ Hz), 7.27 (1H, d, $J=8.2$ Hz) and 7.52 (1H, d, $J=7.8$ Hz). The ^{13}C -NMR spectrum of **2** showed 1 methyl, 9 methylenes, including a methylenedioxy carbon (

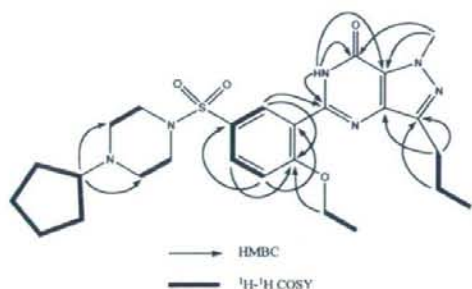


Fig. 4. ^1H - ^1H and Major Long-Range ^1H - ^{13}C Correlations of Compound 1

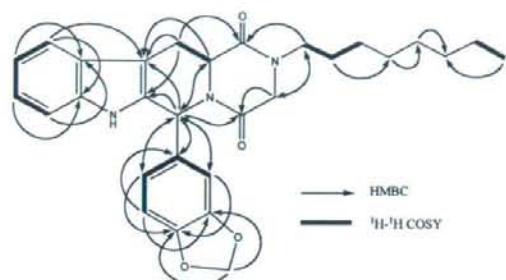


Fig. 5. ^1H - ^1H and Major Long-Range ^1H - ^{13}C Correlations of Compound 2

102.4), 9 methines including 7 aromatic carbons (108.2, 109.0, 111.2, 118.9, 120.3, 121.1, 122.8) and 7 aromatic quaternary carbons (106.1, 127.4, 134.6, 137.6, 138.3, 148.3, 149.2), and 2 carbonyl groups (169.1, 169.6). These signals are very similar to those of tadalafil (Table 2), except for the disappearance of an *N*-methyl group and the presence of 7 methylene signals, including an *N*-methylene group signal at 3.49 (2H, brt, $J=7.4$ Hz) and a methyl signal at 0.89 (3H, t, $J=7.3$ Hz).

Interpretation of the ^1H - ^1H COSY and HMQC spectra of 2 indicated the presence of an *N*-octyl group (Fig. 5). The connectivity of an *N*-octyl group was deduced from the HMBC spectrum (Fig. 5). The methylene proton at 3.49 (H-13) of the *N*-octyl group showed correlations to the carbonyl carbon at 169.1 (C-1) and a methylene carbon at 51.2 (C-3) of tadalafil. Also, methylene protons at 3.94 and 4.24 (H₂-3) showed correlations to the methylene carbon at 47.2 (C-13). These data determined the planar structure of 2, as shown in Fig. 5.

The relative configuration between two methine protons at C-6 and C-12a was established a *cis* configuration by the NOE experiment. Furthermore, the CD spectrum of 2 is superimposable with that of tadalafil (Fig. 6), and it is clear that the absolute stereochemistry of two methine protons at C-6 and C-12a are the same as that of tadalafil. These results enabled us to elucidate the structure of 2 as (6*R*,12*aR*)-6-(1,3-benzodioxol-5-yl)-2-octyl-2,3,6,7,12,12a-hexahydropyrazino[1',2':1,6]pyrdo[3,4-*b*]indol-1,4-dione. The assignments of the ^1H - and ^{13}C -NMR signals of 2 are summarized in Table 2. Considering its properties, compound 2 is designated as *N*-octylnortadalafil.

Table 2. ^1H - and ^{13}C -NMR Chemical Shifts of Compound 2 and Tadalafil in CD_3OD

Position	2 ($^1\text{H}^a$)	Tadalafil ($^1\text{H}^a$)	2 ($^{13}\text{C}^b$)	Tadalafil ($^{13}\text{C}^b$)
1			169.1	168.9
3	4.24 br d (17.4) 3.94 d (17.4)	4.20 br d (17.0) 3.97 d (17.0)	51.2	52.9
4			169.6	169.0
6	6.24 s	6.17 s	57.5	58.0
6a			134.6	134.7
7a			138.3	138.4
8	7.27 d (8.2)	7.25 d (8.3)	111.2	112.2
9	7.07 br t (8.2)	7.06 br t (8.3)	122.8	122.7
10	7.02 br t (7.8)	7.02 br t (7.8)	120.3	120.3
11	7.52 d (7.8)	7.51 d (7.8)	118.9	118.9
11a			127.4	127.4
11b			106.1	106.3
12	3.62 dd (15.6, 5.1) 3.12 br dd (15.6, 11.5)	3.66 dd (15.6, 4.6) 3.11 br dd (15.6, 11.9)	24.2	24.7
12a	4.44 br dd (11.5, 5.1)	4.40 br dd (11.9, 4.6)	57.4	57.6
13 (2H)	3.49 brt (7.4)	3.03 (3H) s	47.2	33.8
14 (2H)	1.59 m		27.9	
15 (2H)	1.30 m		27.8	
16 (2H)	1.26 m		30.4	
17 (2H)	1.32 m		30.4	
18 (2H)	1.28 m		33.0	
19 (2H)	1.31 m		23.7	
20 (3H)	0.89 t (7.3)		14.4	
1'			137.6	137.7
2'	6.78 d (1.9)	6.80 d (1.4)	108.2	108.3
3'			149.2	149.1
4'			148.3	148.2
5'	6.68 d (7.8)	6.68 d (8.2)	109.0	108.9
6'	6.79 dd (7.8, 1.9)	6.82 dd (8.2, 1.4)	121.1	121.3
7' (2H)	5.85 d (6.9)	5.84 d (9.1)	102.4	102.4

a) Recorded in 800 MHz and J values (in Hz) in parentheses. b) Recorded in 200 MHz.

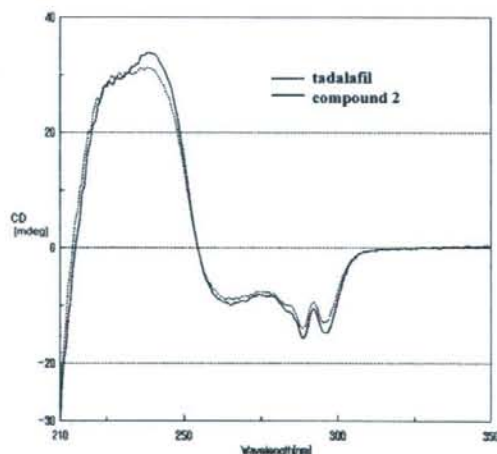


Fig. 6. Overlaid CD Spectra of Tadalafil and Compound 2

Furthermore, quantitative analyses of 1 and 2 in the supplement product were determined by HPLC. The contents of 1 and 2 in the product were about 130 mg/tablet (301 g/mg) and about 27 mg/tablet (64.1 g/mg), respectively.

Finally, we calculated to make docking models of 1 and 2 bound to PDE-5. Compounds 1 and 2 were well fitted to the cavity of PDE-5 like sildenafil and tadalafil, respectively.

Therefore, both compounds are expected to have inhibitory activities against PDE-5.

In conclusion, a new sildenafil analogue, cyclopentynafil and a new tadalafil analogue, *N*-octylnortadalafil were isolated from a dietary supplement illegally marketed in Japan for erectile dysfunction. Their structures were elucidated by using HPLC-PDA, LC-MS, high-resolution MS, NMR and CD. Recently, Toque *et al.* synthesized a new cyclohexyl type of sildenafil analogue and its IC_{50} value as PDE-5 inhibitor was almost same as sildenafil,³⁰ whereas cyclopentynafil and *N*-octylnortadalafil are the first compounds reported to be new sildenafil and tadalafil analogues, respectively, and their inhibitory activities against PDE-5 are expected by docking study. Thus, tremendous risk is faced by patients who unknowingly look to dietary supplements, which are adulterated with such analogues for ED treatment.

Acknowledgement This study was partly supported by a Health and Labour Science Research Grant from the Ministry of Health, Labour and Welfare of Japan.

References

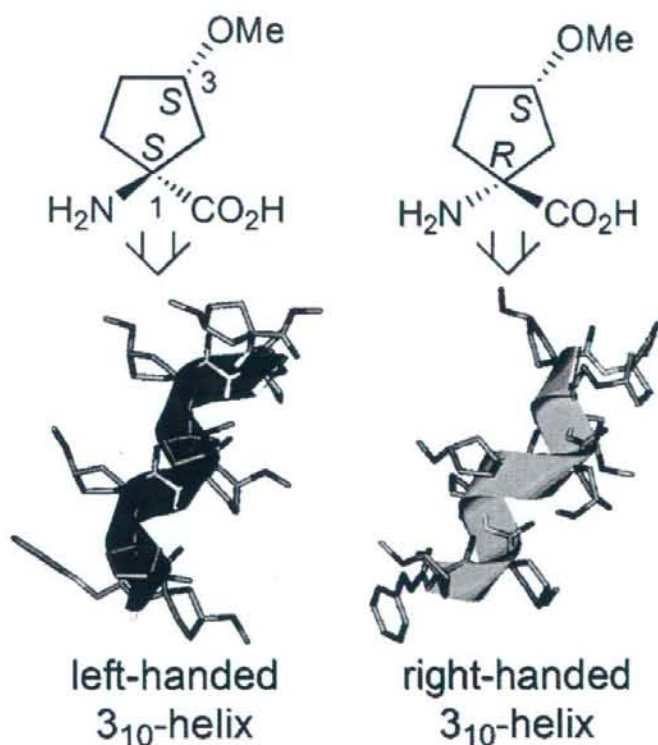
- Ministry of Health, Labour and Welfare of Japan, websites: (<http://www.mhlw.go.jp/kinkyu/diet/other/050623-1.html>)
- Moriyasu T., Shigeoka S., Kishimoto K., Ishikawa F., Nakajima J., Kamimura H., Yasuda I., *Yakugaku Zasshi*, **121**, 765–769 (2001).
- Zhu X., Xiao S., Chen B., Zhang F., Yao S., Wan Z., Yang D., Han H., *J. Chromatogr. A*, **1066**, 89–95 (2005).
- Hasegawa T., Saijo M., Ishii T., Nagata T., Haishima Y., Kawahara N., Goda Y., *J. Food Hyg. Soc. Jpn.*, **49**, 311–315 (2008).
- Jefferson D. R., Natarajan S., Ganesan A., *Synlett*, **2004**, 1428–1430 (2004).
- Venhuis B. J., Barends D. M., Zwaagstra M. E., De Kaste D., "RIVM Report 370030001/2007," National Institute for Public Health and the Environment, the Netherlands, 2007.
- Shin M. H., Hong M. K., Kim W. S., Lee Y. J., Jeoung Y. C., *Food Addit. Contam.*, **20**, 793–796 (2003).
- Shin C., Hong M., Kim D., Lim Y., *Magn. Reson. Chem.*, **42**, 1060–1062 (2004).
- Park H. J., Jeong H. K., Chang M. I., Im M. H., Jeong J. Y., Choi D. M., Park K., Hong M. K., Youm J., Han S. B., *Food Addit. Contam.*, **24**, 122–129 (2007).
- Blok-Tip L., Zomer B., Bakker F., Hartog K. D., Hamzink M., ten Hove J., Vredendregt M., de Kaste D., *Food Addit. Contam.*, **21**, 737–748 (2004).
- Hou P., Zou P., Low M. Y., Chan E., Koh H. L., *Food Addit. Contam.*, **23**, 870–875 (2006).
- Zou P., Hou P., Low M.-Y., Koh H. L., *Food Addit. Contam.*, **23**, 446–451 (2006).
- Zou P., Hou P., Oh S. S., Low M. Y., Koh H. L., *Rapid Commun. Mass Spectrom.*, **20**, 3488–3490 (2006).
- Gratz S. R., Flurer, C. L., Wolnik K. A., *J. Pharm. Biomed. Anal.*, **36**, 525–533 (2004).
- Gratz S. R., Gamble B. M., Flurer R. A., *Rapid Commun. Mass Spectrom.*, **20**, 2317–2327 (2006).
- Lai K. C., Liu Y. C., Tseng M. C., Lin J. H., *J. Food Drug Anal.*, **14**, 19–23 (2006).
- Reepmeyer J. C., Woodruff J. T., *J. Chromatogr. A*, **1125**, 67–75 (2006).
- Reepmeyer J. C., Woodruff J. T., d'Avignon D. A., *J. Pharm. Biomed. Anal.*, **43**, 1615–1621 (2007).
- Reepmeyer J. C., Woodruff J. T., *J. Pharm. Biomed. Anal.*, **44**, 887–893 (2007).
- Lam Y. H., Poon W. T., Lai C. K., Chan A. Y. W., Mak T. W. L., *J. Pharm. Biomed. Anal.*, **46**, 804–807 (2008).
- Zou P., Hou P., Oh S. S., Chong Y. M., Bloodworth B. C., Low M. Y., Koh H. L., *J. Pharm. Biomed. Anal.*, **47**, 279–284 (2008).
- Cho E. Y., Chung S. H., Kim J. H., Kim D. K., Jin C., *J. Appl. Pharmacol.*, **11**, 232–237 (2003).
- Kim J. H., Kim Y., Choi K., Kim D. H., Nam G., Seo J. H., *WO 2002102802* (2002).
- Kumasaka K., Kawahara N., Doi K., Kojima T., Goda Y., *Chem. Pharm. Bull.*, **56**, 227–230 (2008).
- Hosogai N., Hamada K., Tomita M., Nagashima A., Takahashi T., Sekizawa T., Mizutani T., Urano Y., Kuroda A., Sawada K., Ozaki T., Seki J., Goto T., *Eur. J. Pharm.*, **428**, 295–302 (2001).
- Uchiyama N., Saisho K., Kikura-Hanajiri R., Haishima Y., Goda Y., *Chem. Pharm. Bull.*, **56**, 1331–1334 (2008).
- Fujino K., Takami H., Atsumi T., Ogasa T., Mohri S., Kasai M., *Org. Process Res. Dev.*, **5**, 426–433 (2001).
- Onoda Y., Nomoto Y., Ohno T., Yamada K., Ichimura M., *WO9808848* (1998).
- Hirose R., Okumura H., Yoshimatsu A., Irie J., Onoda Y., Nomoto Y., Takai H., Ohno T., Ichimura M., *Eur. J. Pharm.*, **431**, 17–24 (2001).
- Toque F. H. A., Priviero F. B. M., Teixeira C. E., Perissutti E., Fiorino F., Severino B., Frecentese F., Lorenzetti R., Baracat J., Santagada V., Caliendo G., Antunes E., De Nucci G., *J. Med. Chem.*, **51**, 2807–2815 (2008).

Helical-Screw Directions of Diastereoisomeric
Cyclic #-Amino Acid Oligomers

Masanobu Nagano, Masakazu Tanaka, Mitsunobu Doi,
Yosuke Demizu, Masaaki Kurihara, and Hiroshi Suemune

Org. Lett., 2009, 11 (5), 1135-1137 • DOI: 10.1021/ol802963a • Publication Date (Web): 03 February 2009

Downloaded from <http://pubs.acs.org> on April 9, 2009



More About This Article

Additional resources and features associated with this article are available within the HTML version:



ACS Publications
High quality. High impact.

Organic LETTERS

- Supporting Information
- Access to high resolution figures
- Links to articles and content related to this article
- Copyright permission to reproduce figures and/or text from this article

[View the Full Text HTML](#)



ACS Publications

High quality. High impact.

Organic Letters is published by the American Chemical Society, 1155 Sixteenth Street N.W., Washington, DC 20036

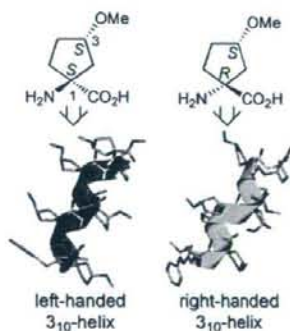
Helical-Screw Directions of Diastereoisomeric Cyclic α -Amino Acid Oligomers

Masanobu Nagano,[†] Masakazu Tanaka,^{*,†,‡} Mitsunobu Doi,[§] Yosuke Demizu,^{||} Masaaki Kurihara,^{||} and Hiroshi Suemune^{*,†}

Graduate School of Pharmaceutical Sciences, Kyushu University, 3-1-1 Maidashi, Higashi-ku, Fukuoka 812-8582, Japan, Graduate School of Biomedical Sciences, Nagasaki University, 1-14 Bunkyo-machi, Nagasaki 852-8521, Japan, Osaka University of Pharmaceutical Sciences, Osaka 569-1094, Japan, and Division of Organic Chemistry, National Institute of Health Sciences, Tokyo 158-8501, Japan
matanaka@nagasaki-u.ac.jp

Received December 24, 2008

ABSTRACT



Two series of homooligomers composed of diastereoisomeric cyclic α -amino acids having two chiral centers at the α -carbon and the side chain were synthesized, and their preferred secondary structures were studied in solution and in the crystal state. The oligomers are a new class of helical-foldamers possessing two kinds of chiral centers on the helical backbone and at the lateral surface of the helix.

Right-handed α -helical-screw structures in proteins are believed to result from the L-(S)-chiral α -carbon atoms on the peptide backbone.¹ Recently, Toniolo's group and we independently reported that the helical-screw sense of peptide-oligomers can be controlled without a chiral center on the peptide backbone, but by chiral centers at the side chain.² However, so far, little attention has been paid to how both chiral centers on the peptide backbone and at the side

chain influence the secondary structures of their oligomers.³ Herein, we designed two diastereoisomeric cyclic amino

(2) (a) Tanaka, M.; Demizu, Y.; Doi, M.; Kurihara, M.; Suemune, H. *Angew. Chem., Int. Ed.* 2004, 43, 5360–5363. (b) Tanaka, M.; Anan, K.; Demizu, Y.; Kurihara, M.; Doi, M.; Suemune, H. *J. Am. Chem. Soc.* 2005, 127, 11570–11571. (c) Royo, S.; Borggraeve, W. M. D.; Peggion, C.; Formaggio, F.; Crisma, M.; Jiménez, A. I.; Cativiela, C.; Toniolo, C. *J. Am. Chem. Soc.* 2005, 127, 2036–2037.

(3) (a) Jiménez, A. I.; Cativiela, C.; Aubry, A.; Marraud, M. J. *Am. Chem. Soc.* 1998, 120, 9452–9459. (b) Sharma, G.; Reddy, K. R.; Krishna, P. R.; Sankar, A. R.; Jayaprakash, P.; Jagannadh, B.; Kunwar, A. C. *Angew. Chem., Int. Ed.* 2004, 43, 3961–3965. (c) Andreetto, E.; Peggion, C.; Crisma, M.; Toniolo, C. *Biopolymers (Peptide Sci.)* 2006, 84, 490–501. (d) Kúmin, M.; Sonntag, L.-S.; Wennemers, H. *J. Am. Chem. Soc.* 2007, 129, 466–467.

[†] Kyushu University.

[‡] Nagasaki University.

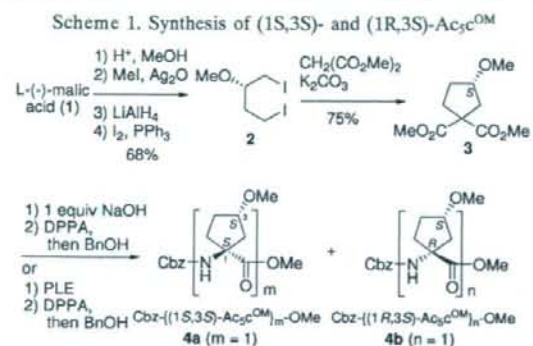
[§] Osaka University of Pharmaceutical Sciences.

^{||} National Institute of Health Sciences.

(1) Branden, C.; Tooze, J. *Introduction to Protein Structure*; Garland: New York, 1991; pp 1–31.

acids,⁴ (1*S*,3*S*)- and (1*R*,3*S*)-1-amino-3-(methoxy)cyclopentanecarboxylic acids ($\text{Ac}_5\text{c}^{\text{OM}}$), constructed their homooligomers having chiral centers both on the peptide-backbone and at the side chain, and revealed their unique helical structures with high resolution analyses.

Two cyclic amino acids (1*S*,3*S*)- $\text{Ac}_5\text{c}^{\text{OM}}$ and (1*R*,3*S*)- $\text{Ac}_5\text{c}^{\text{OM}}$ were synthesized starting from L-(–)-malic acid **1** (Scheme 1). After esterification of **1**, the secondary alcohol



was converted to a methyl ether. Then, reduction of diester followed by iodination of alcohol gave a diiodide **2**. Dialkylation of dimethyl malonate with **2** afforded a cyclopentane diester **3**. Monohydrolysis of **3** with an alkaline solution, followed by Curtius rearrangement with diphenylphosphoryl azide (DPPA), produced two separable diastereoisomers (1*S*,3*S*)- $\text{Ac}_5\text{c}^{\text{OM}}$ (**4a**) and (1*R*,3*S*)- $\text{Ac}_5\text{c}^{\text{OM}}$ (**4b**) in a ratio of 3:1 in 85% yield.⁵ Meanwhile, hydrolysis of **3** with pig liver esterase (PLE) followed by Curtius rearrangement could change the diastereoselectivity (**4a**:**4b** = 1:2; 84% yield). The stereochemistry of products was unambiguously assigned by the X-ray crystallographic analyses of their oligomers.⁶

Oligomers $\text{Cbz}-\{(1*S*,3*S*)-\text{Ac}_5\text{c}^{\text{OM}}\}_m\text{-OMe}$ ($m = 2$ (**5a**), **4** (**7a**), **6** (**8a**), **8** (**9a**), **10** (**10a**)) and $\text{Cbz}-\{(1*R*,3*S*)-\text{Ac}_5\text{c}^{\text{OM}}\}_n\text{-OMe}$ ($n = 2$ (**5b**), **3** (**6b**), **4** (**7b**), **6** (**8b**), **8** (**9b**), **10** (**10b**)) were generally prepared by the coupling between N-terminal-free oligomers and N-protected dipeptide acid via solution-phase methods. It should be noted that elongation of N-terminal-free (1*R*,3*S*)- $\text{Ac}_5\text{c}^{\text{OM}}$ dimer to a tetramer **7b** did not work well because diketopiperazine was formed as a byproduct. Thus, the (1*R*,3*S*)-tetramer was prepared via a trimer **6b**, which was derived from an N-terminal-free amino acid and the dipeptide acid.⁶

The FT-IR absorption spectra of both (1*S*,3*S*)- and (1*R*,3*S*)- $\text{Ac}_5\text{c}^{\text{OM}}$ oligomers in CDCl_3 solution showed weak bands in the region $3420\text{--}3430\text{ cm}^{-1}$ [free (solvated) peptide NH

groups] and strong bands at $3320\text{--}3380\text{ cm}^{-1}$ (intramolecularly H-bonded peptide NH groups). The latter bands observed at 3380 cm^{-1} in **5a** and at 3376 cm^{-1} in **5b** shift to lower wavenumbers (3320 cm^{-1} in **10a** and 3320 cm^{-1} in **10b**), respectively, and the relative intensities increase with elongation of the peptide length. These IR spectra are very similar to those of helical $\text{Ac}_5\text{c}^{\text{OM}}$ oligomers.⁷

In the ROESY ^1H NMR spectra, the hexamers **8a** and **8b** showed a complete series of sequential d_{NN} cross-peaks of NOEs from the N-terminal NH(1) to the C-terminal NH(6), respectively.⁶ These correlations are characteristic for the helical structure, albeit that those of longer oligomers only gave a partial series of sequential d_{NN} cross-peaks. Addition of DMSO or the free-radical TEMPO in the ^1H NMR spectroscopy indicated that the two NH signals [NH(1) and NH(2)] at the N-terminus of (1*R*,3*S*)-oligomers **8b** and **9b** are sensitive (solvent-exposed NH group), respectively, suggesting that the two NH groups are not intramolecularly H-bonded, and formation of a helical structure.^{2,6,7} The experiments of (1*S*,3*S*)-oligomers **8a** and **9a** did not give clear results because the relevant NH peaks overlapped.⁶

The CD spectra of tetramers **7** and hexamers **8** in 2,2,2-trifluoroethanol (TFE) solution, both (1*S*,3*S*)- and (1*R*,3*S*)- $\text{Ac}_5\text{c}^{\text{OM}}$, did not show characteristic maxima (208 and 222 nm) for the helical structure. These spectra may suggest the presence of both right-handed (P) and left-handed (M) helices or disordered structures. Elongation of oligomer length changed the shapes of CD spectra, and positive maxima at 208 and 222 nm were observed in the (1*S*,3*S*)-octamer **9a** and decamer **10a** while negative maxima were seen in the (1*R*,3*S*)-**9b** and **10b**. These CD spectra suggest that the dominant conformation of (1*S*,3*S*)-**9a** and **10a** is a left-handed (M) helix and that of (1*R*,3*S*)-**9b** and **10b** is a right-handed (P) helix. The CD spectra of (1*S*,3*S*)- and (1*R*,3*S*)-oligomers showed a pseudosymmetric shape, strongly indicating that the CD curves are the result of approximately enantiomeric global chain helicity (Figure 1).

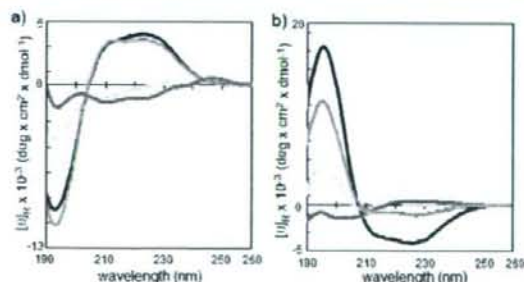


Figure 1. CD spectra of (1*S*,3*S*)- and (1*R*,3*S*)-oligomers in TFE solution (100 μM). (a) **7**–**10a**: $\text{Cbz}-\{(1*S*,3*S*)-\text{Ac}_5\text{c}^{\text{OM}}\}_m\text{-OMe}$ ($m = 4, 6, 8, 10$). (b) **7**–**10b**: $\text{Cbz}-\{(1*R*,3*S*)-\text{Ac}_5\text{c}^{\text{OM}}\}_n\text{-OMe}$ ($n = 4, 6, 8, 10$). Tetramer **7** (green), hexamer **8** (yellow), octamer **9** (blue), and decamer **10** (red).

The X-ray analysis of (1*S*,3*S*)- $\text{Ac}_5\text{c}^{\text{OM}}$ hexamer **8a** having 12 chiral centers showed both diastereomeric right-handed

(4) (a) Cativiela, C.; D-de-Villegas, M. D. *Tetrahedron: Asymmetry* 2000, 11, 645–732. (b) Kotha, S. *Acc. Chem. Res.* 2003, 36, 342–351.

(5) Nagano, M.; Demizu, Y.; Tanaka, M.; Kurihara, M.; Doi, M.; Suemura, H. *Peptide Science 2005*; The Japanese Peptide Society: Osaka, Japan, 2006; pp 345–346.

(6) See the Supporting Information.

(P) and left-handed (M) 3_{10} -helices (Figure 2). In contrast, (1S,3S)-octamer 9a crystallized exclusively to left-handed

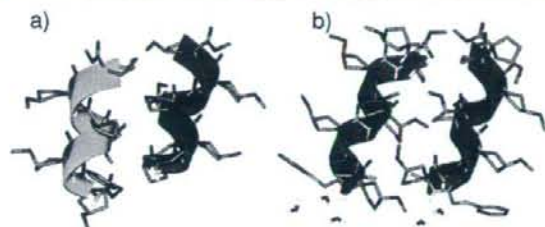


Figure 2. X-ray crystallographic analysis of Cbz-((1S,3S)-Ac₅c^{OM})_m-OMe [(a) 8a: m = 6, (b) 9a: m = 8]. Red: left-handedness (M), blue: right-handedness (P).

(M) 3_{10} -helices, while in the asymmetric unit there were two crystallographically independent (M) 3_{10} -helical conformers. The diastereomeric (1R,3S)-Ac₅c^{OM} hexamer 8b showed two crystallographically independent right-handed (P) 3_{10} -helices. The (1R,3S)-octamer 9b also showed two conformers, both (P) 3_{10} -helices but in the one conformer the signs of ϕ , ψ torsion angles at the C-terminal residue were opposite. There, six consecutive intramolecular H-bonds of the $i-i+3$ type ($i = 0\sim 5$) were found, respectively.^{6,8}

In the crystal state, the (1S,3S)-hexamer 8a having 12 chiral centers at the α -carbon and the side chain assumed both (P) and (M) 3_{10} -helices,^{2b} while the (1R,3S)-hexamer 8b formed only (P) helices, probably influenced by the crystal packing force. By the elongation of peptide length, i.e., by the increase of chiral centers, both (1S,3S)- and (1R,3S)-oligomers were controlled to form one-handed helical-screw structures in solution and in the crystal state; i.e., the (1S,3S)-octamer 9a formed (M) helices and the (1R,3S)-octamer 9b formed (P) helices. Molecular mechanics/ab initio (RHF/3-21G*) calculations of (1S,3S)-9a produced a (M) 3_{10} -helix as a global minimum-energy (GME) conformation, and those of (1R,3S)-9b gave a (P) 3_{10} -helix as a GME conformation.⁶

At first, we considered each effect of the α -carbon and the side-chain chiral centers or match/mismatch of chiral centers on one-handed helical-screw direction. However, the

(7) (a) Santini, A.; Barone, V.; Bavoso, A.; Benedetti, E.; Di Blasio, B.; Fraternali, F.; Leij, F.; Pavone, V.; Pedone, C.; Crisma, M.; Bonora, G. M.; Toniolo, C. *Int. J. Biol. Macromol.* 1988, 10, 292–299. (b) Crisma, M.; Bonora, G. M.; Toniolo, C.; Benedetti, E.; Bavoso, A.; Di Blasio, B.; Pavone, V.; Pedone, C. *Int. J. Biol. Macromol.* 1988, 10, 300–304.

(8) In some oligomers, inversions of signs or distortions of ϕ , ψ torsion angles at the C-terminal residue are observed. See the Supporting Information.

(9) (a) Gellman, S. H. *Acc. Chem. Res.* 1998, 31, 173–180. (b) Seebach, D.; Beck, A. K.; Bierbaum, D. J. *Chem. Biodiversity* 2004, 1, 1111–1239. (c) Wu, C. W.; Kirshenbaum, K.; Sanborn, T. J.; Patch, J. A.; Huang, K.; Dill, K. A.; Zuckermann, R. N.; Barron, A. E. *J. Am. Chem. Soc.* 2003, 125, 13525–13530. (d) Toniolo, C.; Crisma, M.; Formaggio, F.; Peggion, C.; Broxterman, O. B.; Kaptein, B. *Biopolymers (Peptide Sci.)* 2004, 76, 162–176. (e) Toniolo, C.; Formaggio, F.; Kaptein, B.; Broxterman, O. B. *Synlett* 2006, 1295–1310. (f) Tanaka, M. *Chem. Pharm. Bull.* 2007, 55, 349–358. (g) Maity, P.; König, B. *Biopolymers (Peptide Sci.)* 2008, 90, 8–27.

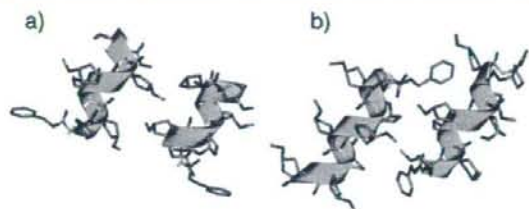


Figure 3. X-ray crystallographic analysis of Cbz-((1R,3S)-Ac₅c^{OM})_n-OMe [(a) 8b: n = 6, (b) 9b: n = 8].

Ac₅c^{OM} possess a unique chiral structure; i.e., transfer of the MeO-substituent on the γ -positions of cyclopentane in (1S,3S)-4a results in formation of enantiomer (1R,3R) or diastereomer (1R,3S) because the chirality of the α -carbon (C1) is changed (Figure 4). Thus, the helical-screw structures

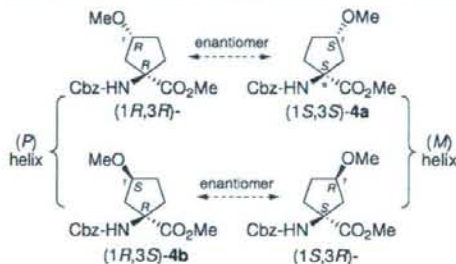


Figure 4. Unique chiral structure of Ac₅c^{OM} and helical-screw direction of their oligomers.

might be controlled by the whole chiral cyclopentane amino acid structure.

In summary, we synthesized two series of the diastereomeric Ac₅c^{OM} oligomers that are a new class of helical-foldamers possessing two kinds of chiral centers on the helical backbone and at the lateral surface of the helix⁹ and revealed their preferred helical conformations in solution and in the crystal state. These results might be useful for design of foldamer catalysts and lead compounds, which are currently under investigation in our group.

Acknowledgment. This work was in part supported by Grant-in-Aid (B) from JSPS, by a Grant-in Aid for Scientific Research on Priority Areas (No. 20037054, “Chemistry of Concerto Catalysis”) from MEXT, and also by a Grant-in-Aid from the ASAHI GLASS Foundation. M.N. thanks the JSPS for Research Fellowships.

Supporting Information Available: Experimental section, spectroscopic data of new compounds, crystallographic details (CIF), and molecular calculations. This material is available free of charge via the Internet at <http://pubs.acs.org>.

OL802963A

Computational Study on Helical Structure of α,α -Disubstituted Oligopeptides Containing Chiral α -Amino Acids

Masaaki Kurihara¹, Yukiko Sato¹, Nanako Yamagata¹, Haruhiro Okuda¹,
Masanobu Nagano², Yosuke Demizu², Mitsunobu Doi³, Masakazu Tanaka²,
Hiroshi Suemune²

¹Division of Organic Chemistry, National Institute of Health Sciences, Tokyo 158-8501, Japan, ²Graduate School of Pharmaceutical Sciences, Kyushu University, Fukuoka 812-8582, Japan, ³Osaka University of Pharmaceutical Sciences, Osaka 569-1094, Japan

email: masaaki@nihs.go.jp

Computational simulation using conformational search calculations with AMBER force field is most useful for conformational analysis of oligopeptides containing α,α -disubstituted α -amino acids. The results were in agreement with those of x-ray and were most stable conformation evaluated by molecular orbital calculation.*

Keywords: α,α -disubstituted α -amino acid, oligopeptide, conformational search, MacroModel, molecular orbital calculation

Introduction

We have studied on the conformational search of ligands in receptor or enzyme with AMBER* force field. [1-2] Prediction of the conformation of oligopeptides using computational simulation presents an interesting challenge to design functionalized and bioactive peptides. We have shown that the Monte Carlo conformational search method using MacroModel is useful to predict helical structures (α -helix, 3_{10} -helix) of oligopeptides prepared from α,α -disubstituted α -amino acids. Moreover, we have studied conformational analysis of oligopeptides containing chiral α,α -disubstituted α -amino acids to predict the helical screw sense of helical structures. [3-6]

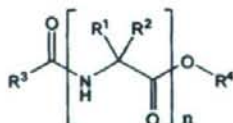
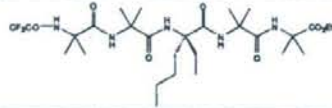
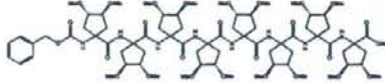
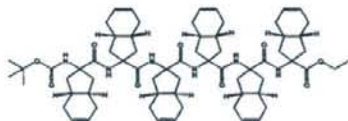


Fig. 1. Structures of α,α -disubstituted oligopeptides.

Results and Discussion

We calculated α,α -disubstituted peptide using MCMM conformational search with various force fields (AMBER*, MMFF, OPLS) and showed the results in Table 1. In the case of using AMBER* force field the results were in agreement with those of x-ray and were most stable conformation evaluated by 3-21G level molecular orbital calculation. These results indicated that computational simulation using conformational search calculations with AMBER* force field is most useful for conformational analysis of oligopeptides containing α,α -disubstituted α -amino acids.

Table 1. conformational analysis of oligopeptides containing α,α -disubstituted α -amino acids

Peptides	Global Minimum			X-ray
	By MacroModel/MCMM Conformational Search			
	AMBER*	MMFF	OPLS	
	(P)-3 ₁₀ -helix	Random coil	Random coil	(P)-3 ₁₀ -helix
	3-21G by Spartan			
	0 (kcal/mol)	+14.09	+16.83	
	(M)- α -helix	(M)- α ,3 ₁₀ -helix	(M)- α -helix	(M)- α -helix
	3-21G by Spartan			
	0 (kcal/mol)	+13.52	+9.32	
	(P)-3 ₁₀ -helix	(P)- α ,3 ₁₀ -helix	(M)- α -helix	(P),(M)-3 ₁₀ -helix
	3-21G by Spartan			
	0 (M+1.14)	+14.28	+20.67	

Acknowledgement

This work was supported in part by the Budget for Nuclear Research of the Ministry of Education, Culture, Sports, Science and Technology, based on the screening and counseling by the Atomic Energy Commission and by a Grant-in-Aid for Scientific Research (C) from the Japan Society for the Promotion of Science.

References

- Hakamata, W., Sato, Y., Okuda, H., Honzawa, S., Saito, N., Kishimoto, S., Yamamoto, A., Sugiura, T., Kittaka, A., Kurihara, M. (2008) *Bioorg. Med. Chem. Lett.*, **18**, 120-123
- Kurihara, M., Rouf, A. S. S., Kansui, H., Kagechika, H., Okuda, H., Miyata, N. (2004) *Bioorg. Med. Chem. Lett.*, **14**, 4131-4134
- Kurihara, M., Sato, S., Kaneko, F., Okuda, H., Nagano, M., Demizu, Y., Doi, M., Tanaka, M., Suemune, H. (2008) *Peptide Science 2007*, 137-138.
- Demizu, Y., Tanaka, M., Nagano, M., Kurihara, M., Doi, M., Maruyama, T., Suemune, H. (2007) *Chem. Pharm. Bull.*, **55**, 840-842.
- Kurihara, M., Sato, Y., Hakamata, W., Okuda, H., Nagano, M., Hama, M., Demizu, Y., Doi, M., Tanaka, M., Suemune, H. (2006) *Peptide Science 2006*, 88.
- Tanaka, M., Anan, K., Demizu, Y., Kurihara, M., Doi, M., Suemune, H. (2005) *J. Am. Chem. Soc.*, **127**, 11570-11571.

Design and Synthesis of Chiral Cyclic α,α -Disubstituted Amino Acid Having Azido Functions, and Its Oligopeptides

Hiroomi Takazaki¹, Masakazu Tanaka¹, Naomi Kawabe¹, Masanobu Nagano¹, Mitsunobu Doi², Masaaki Kurihara³, and Hiroshi Suemune¹

¹Graduate School of Pharmaceutical Sciences, Kyushu University, 3-1-1 Maidashi, Higashi-ku, Fukuoka 812-8582, Japan, ²Osaka University of Pharmaceutical Sciences, Osaka 569-1094, Japan, ³Division of Organic Chemistry, National Institute of Health Sciences, Tokyo 158-8501, Japan
e-mail: matanaka@nagasaki-u.ac.jp

We designed and synthesized a chiral cyclic α,α -disubstituted α -amino acid having azido functions: $\{(3R,4R)$ -1-amino-3,4-diazidocyclopentanecarboxylic acid; (R,R) -Ac₅c^{dn3} $\}$, and studied the preferred secondary structure of its homopeptides. Furthermore, the azido functions in the cyclic amino acid (R,R) -Ac₅c^{dn3} could be converted into various functional groups.

Keywords: azido functions, cyclic amino acid, α,α -disubstituted α -amino acid, peptide conformation, chiral center

Introduction

Helices in proteins almost always show a right-handed (*P*) helical screw, which is believed to result from the asymmetric center at the α -position of L- α -amino acids. We have previously reported that the side-chain chiral centers of amino acid affect the secondary structures of their peptides [1]; that is to say, we synthesized a chiral cyclic α,α -disubstituted α -amino acid; (S,S) -Ac₅c^{dom}, in which the α -carbon atom is not a chiral center but asymmetric centers exist at the side chain. The (S,S) -Ac₅c^{dom} homopeptides preferentially formed a left-handed helical screw from the side-chain chiral centers (Fig. 1).

Herein, we designed a chiral cyclic amino acid with azido functions; $(3R,4R)$ -1-amino-3,4-diazidocyclopentanecarboxylic acid $\{(R,R)$ -Ac₅c^{dn3} $\}$, in which azido functions were thought to be easily converted into various functional groups. Moreover, we prepared homopeptides composed of (R,R) -Ac₅c^{dn3}, and studied the preferred conformation of peptides.



Fig. 1. Helical structure of (S,S)-Ac₅c^{dOM} octapeptide.

Results and Discussion

We synthesized a chiral cyclic amino acid (*R,R*)-Ac₅c^{dN₃} starting from dimethyl L-(+)-tartrate (Fig. 2). After conversion of dimethyl L-(+)-tartrate to diiodide (1), dimethyl malonate was bisalkylated with diiodide 1 to give a cyclic diester (2). Deprotection of the MOM ether, conversion of diol to diazido function, monohydrolysis of diester, and subsequent Curtius rearrangement afforded the chiral cyclic amino acid (*R,R*)-Ac₅c^{dN₃}. Azido functions in the amino acid could be easily converted into amino functions by reduction, triazole functions by the “click” reaction, and amide functions by reduction and acylation.

We prepared homopeptides composed of (*R,R*)-Ac₅c^{dN₃} by solution-phase methods, and studied the preferred secondary structure of peptides in solution. FT-IR and the ROESY ¹H NMR spectra indicated that (*R,R*)-Ac₅c^{dN₃} homopeptides preferentially formed a helical structure in CDCl₃ solution. Now we are studying the preferred secondary structure of peptides in the crystal state by X-ray crystallographic analysis.

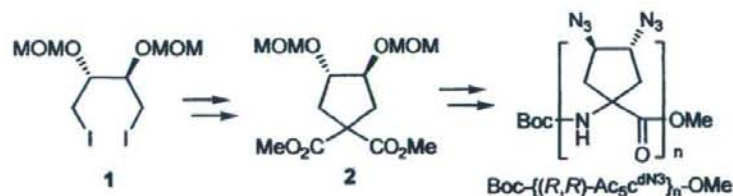


Fig. 2. Synthesis of (*R,R*)-Ac₅c^{dN₃} and its homopeptides.

Acknowledgments

This work was supported in part by a Grant-in-Aid (B) from JSPS, a Grant-in-Aid for Scientific Research on Priority Areas (No. 20037054, “Chemistry of Concerto Catalysis”) from MEXT, and a Grant-in-Aid from the ASAHI GLASS Foundation. The present address of Y.D. and M.T. is Nagasaki University.

References

- a) Tanaka, M., Demizu, Y., Doi, M., Kurihara, M., Suemune, H. (2004) *Angew. Chem. Int. Ed.*, **43**, 5360-5363; b) Tanaka, M. (2007) *Chem. Pharm. Bull.*, **55**, 349-358.

Cooperative Strand Invasion by Peptide Nucleic Acid

Toru Sugiyama¹, Yasutada Imamura², Masaaki Kurihara³, and Atsushi Kittaka⁴

¹Department of Life Sciences, Graduate School of Arts and Sciences, The University of Tokyo, Komaba, Meguro-ku, Tokyo 153-8902, Japan, ²Faculty of Engineering, Kogakuin University, 2665-1 Nakano, Hachioji, Tokyo 192-0015, Japan, ³Division of Organic Chemistry, National Institute of Health Sciences, Ministry of Health and Welfare, Kamiyoga, Setagaya-ku, Tokyo 158-8501, Japan and ⁴Faculty of Pharmaceutical Sciences, Teikyo University, Sagamiko, Kanagawa 199-0195, Japan
email: csugi@mail.ecc.u-tokyo.ac.jp

Peptide nucleic acid (PNA) is a synthetic DNA/RNA mimic in which the sugar-phosphate backbone is replaced by a peptide backbone. A remarkable feature of PNA is its ability to recognize sequences within duplex DNA by strand invasion. In order to improve DNA binding properties of PNA, we tested the effect of cooperativity on triplex invasion. We here demonstrate that a PNA targeting six bases cooperatively strand invades into duplex DNA with excellent sequence specificity.

Keywords: antigene, cooperativity, peptide nucleic acid

Introduction

Among the numerous methods for DNA recognition, of particular interest is strand invasion by peptide nucleic acid (PNA). PNA is one of the most successful analogues of oligonucleotides with potential applications in antisense and antigene strategy [1]. Strand invasion can occur via several distinct mechanisms: triplex invasion, double-duplex invasion, and duplex invasion. Among them most studies have focused on triplex invasion by using homopyrimidine PNAs, because a number of oligonucleotide-dependent enzymatic reactions are inhibited by PNA, including transcription and translation. Recognition of a unique site in the human genome requires discrimination of a specific sequence of 15-16 base pairs from all other possible sequences. However, the affinity of even relatively short bis-PNAs (8-10 bases) to their target sites is so high that PNA binding to correct and even to mismatched sites is virtually irreversible. In this regard, sequence-specificity of PNA triplex invasion is limited and this limitation hinders its application in living cells. As a possible mechanism for improving the specificity of strand invasion, we tested whether PNAs could cooperatively invade into a duplex DNA.

Results and Discussion

A hexameric bis-PNA, PNA 1, was used to test the effect of cooperative binding interaction on triplex invasion (Fig. 1). The purine target sequence

5'-GA₁₀G-3' can be considered as two contiguous target sites, 5'-GA₅-3' and 5'-A₅G-3' (Fig. 2).

Figure 2 shows the results of the gel mobility shift assay. PNA 1 incubated with D^M generated no detectable band. A similar result was observed for D^D(4). This suggests that this short pyrimidine PNA 1 has low binding affinity for their target sites that are isolated or separated by 4 nucleobases. The PNA molecules are rapidly displaced by the internal competing complementary DNA strand during electrophoresis. In contrast, when PNA 1 was incubated with D^D(0), clear bands corresponding to triplex invasion complexes were observed. This marked improvement of the binding efficiency indicates a positive binding interaction between contiguous PNAs, aligned head to head in the invasion complex (Fig. 1).

The sequence specificity of PNA 1 was examined by comparing its affinity for fully matched 12 base pair target to that for a sequence containing a single-base mismatch, D^Dmis. PNA 1 displayed excellent specificity in an all-or-none manner. Since each PNA molecule is bound to a short DNA target, a single mismatched base pair destabilizes such a complex to a large extent, thus destabilizing the whole invasion complexes. Consequently, high specificity was realized.

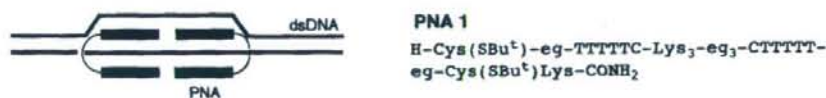


Fig. 1. Schematic representation of cooperative strand invasion of dsDNA by PNA (left) and the sequence of PNA used in this study (right). eg denotes 8-amino-2,6-dioxaoctanoic acid unit.

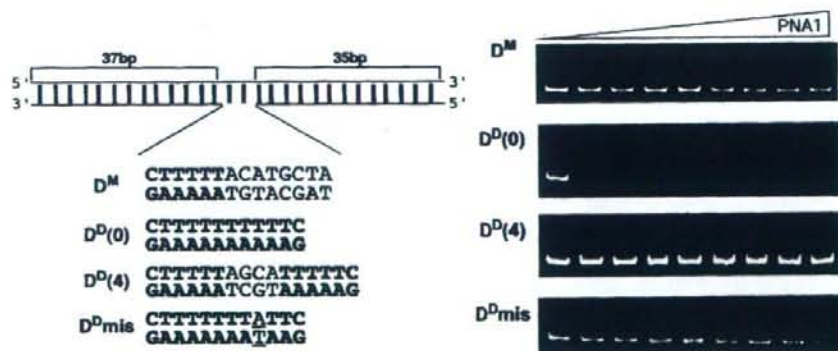


Fig. 2. An illustration of dsDNA used in this study (left) and the results of polyacrylamide gel mobility shift assay (right). PNA concentrations were 0, 1, 1.3, 1.8, 2.4, 3.2, 4.2, 5.6, and 7.5 μ M, respectively.

Reference

- Nielsen, P. E., Egholm, M., Berg, R. H., and Buchard, O. (1991) *Science*, **254**, 1479-1500.